Supporting Information

Encapsulation of N-containing compounds in a new hydrophilic Cd-based crystalline sponge via Coordinative Alignment Method

Faiza Habib[a]*, Derek A. Tocher[a], and Claire J. Carmalt[a]

[a]Department of Chemistry, University College London, 20 Gordon Street, London, WC1H 0AJ, U.K.

Corresponding Author Address: UCL Department of Chemistry, 20 Gordon Street, London, WC1H 0AJ.

Tel: +44 7440171357.

Email: faiza.habib@ucl.ac.uk

Contents

S1. Geometry of Cd1-Cd7 ions in sponge 2

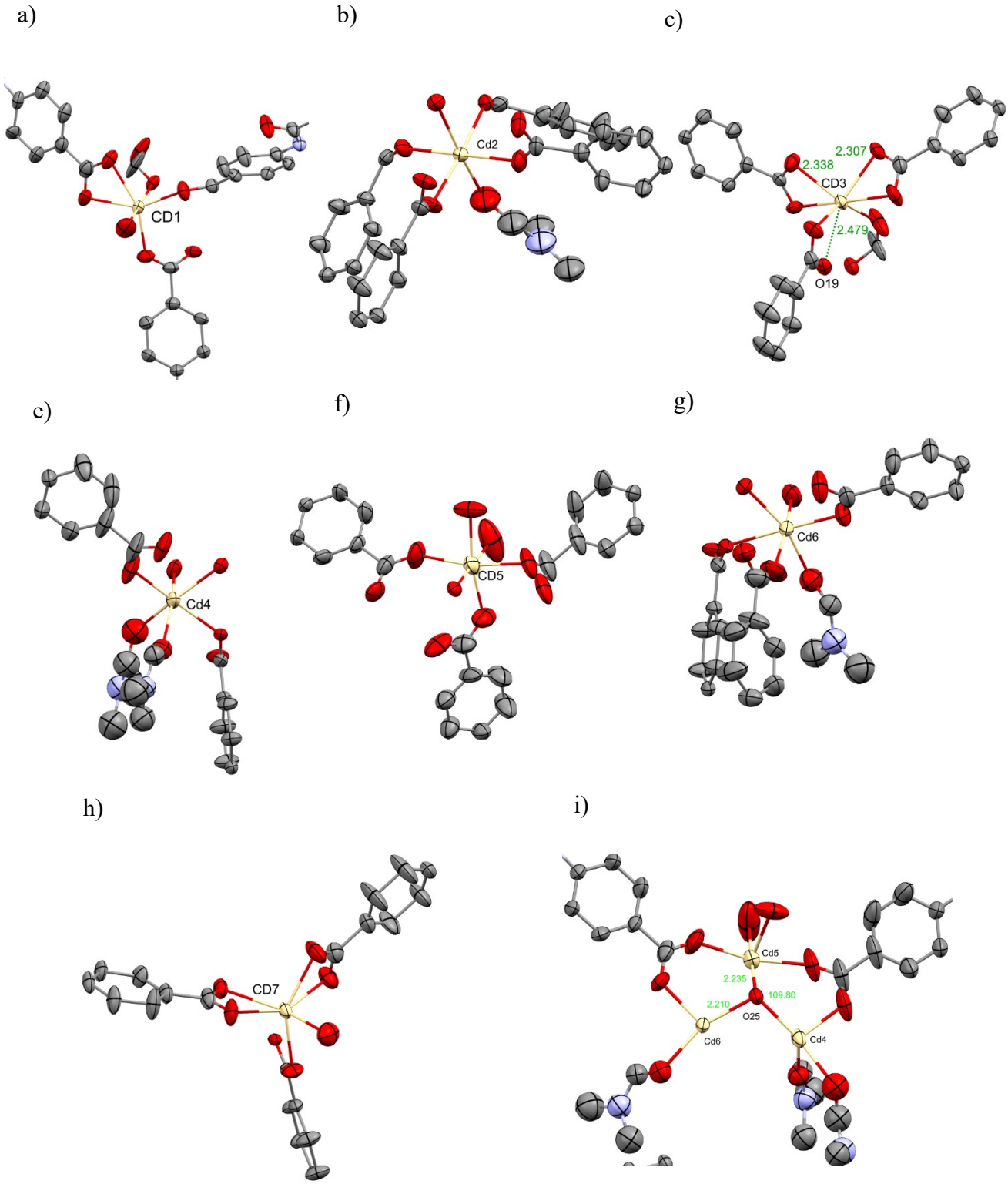

Figure S 1. a)-g) Geometry of Cd1-Cd7 ions surrounded by linker molecules, OH^- ligands, water molecules and DMF molecules. Framework displayed in ellipsoids at 50% probability.

S2. Optimisation of Conditions of Encapsulation of Guests A, B and C in sponge 2.

SCXRD analysis of **2** shows that DMF molecules from the synthesis were coordinated to the Cd ions. Several attempts were made to remove DMF from the pores as well from the coordination site by solvent exchange with methanol, ethanol, isopropanol, chloroform, acetonitrile, acetone, and pyridine. Exchange with neat chloroform and neat methanol resulted in the deterioration of the crystals. The crystals were severely damaged with multiple cracks developed and the crystal were broken in several small pieces therefore, unsuitable for X-ray measurement. The crystals survived in neat ethanol, acetone, isopropanol, and acetonitrile. SCXRD analysis revealed that solvents partially removed DMF from the pores however DMF remained bonded to the metal ions.

S3. Synthesis of sponge 3

Sponge **3** was obtained when crystals of **2** were exchanged with diluted pyridine. When neat pyridine was used the crystal dissolved therefore pyridine was diluted with DMF. SCXRD analysis revealed that pyridine molecules replaced DMF from the coordination site but one coordinated DMF was remaining. Therefore, acetone for dilution was selected and results revealed that pyridine successful replaced DMF from all the coordination sites which is the formation of sponge **3**. Details of solvent exchange are represented in Table S1

*Table S 1. Soaking conditions of crystals **2** in various solvents.*

Solvent	Composition	Incubation period/days	Results
Methanol	neat	2	Cracks start appearing in the crystals as soon as removed from the solvent and crystal lost its crystallinity therefore data could not be collected
Chloroform	neat	2	Cracks developed into the crystals soon after exposure to the solvent and crystals were broken into many small pieces unsuitable for x-ray measurement.
Ethanol	neat	2	Crystals remain stable. SCXRD analysis showed ethanol molecules in the pores along with a few DMF molecules.
Ethanol	neat	14	Crystals optically look fine but do not diffract.
Acetonitrile (**A**)	neat	3	Crystals remain stable. SCXRD analysis showed acetonitrile molecules in the pores along with DMF molecules. Inclusion complex **2A**
Acetonitrile	neat	30	Crystals remain stable. SCXRD analysis showed acetonitrile molecules in the pores along with a few DMF molecules.
Acetone (**B**)	neat	7	Crystals remain stable. SCXRD analysis showed acetone molecules in the pores along with a few DMF molecules. Inclusion complex **2B**
Acetone	neat	30	Crystals remain stable. SCXRD analysis showed acetone molecules in the pores along with a few DMF molecules
Isopropanol (**C**)	neat	8	Crystals remain stable. SCXRD analysis showed isopropanol molecules in the pores along with a few DMF molecules. Inclusion complex **2C**
Isopropanol	neat	21	Crystals optically look fine but do not diffract.
Pyridine	neat	1	Crystal dissolved
Pyridine	Pyridine (50 µL) DMF (3 mL)	7	Out of 6 Coordinated DMF molecules, pyridine replaced 5 DMF molecules. However, one DMF was still coordinated to the Cd.
Pyridine	Pyridine (50 µL) Acetone (3 mL)	14	All coordinated DMF molecules were replaced by the pyridine molecules. Acetone and DMF molecules were observed in the pores. Inclusion complex **3**

S4. Host-guest interactions

i) Intermolecular interaction between DMF molecules in the pore and sponge 2

In the asymmetric unit of sponge **2**, there were six DMF in the pores. Figure S2a-d illustrates the intermolecular interactions between the host framework and DMF molecules. Guest molecules were coloured according to the positional equivalence in the structure. It was observed that the DMF molecules identified in blue, turquoise, red, green and pink are strongly bonded to the framework via hydrogen bonds. These particular sites were consistently occupied either by the DMF molecules or replaced by the incoming guest in the inclusion complexes **2A**, **2B** and **2C**. It is important to recognise these favourable sites and identify the type of intermolecular interaction between the host and DMF molecules. The above observations indicated that sponge **2** behaved as a hydrophilic sponge and hydrogen bonding was identified as the dominant host-guest interaction. Therefore, it was expected that sponge **2** may accommodate a number of polar solvents.

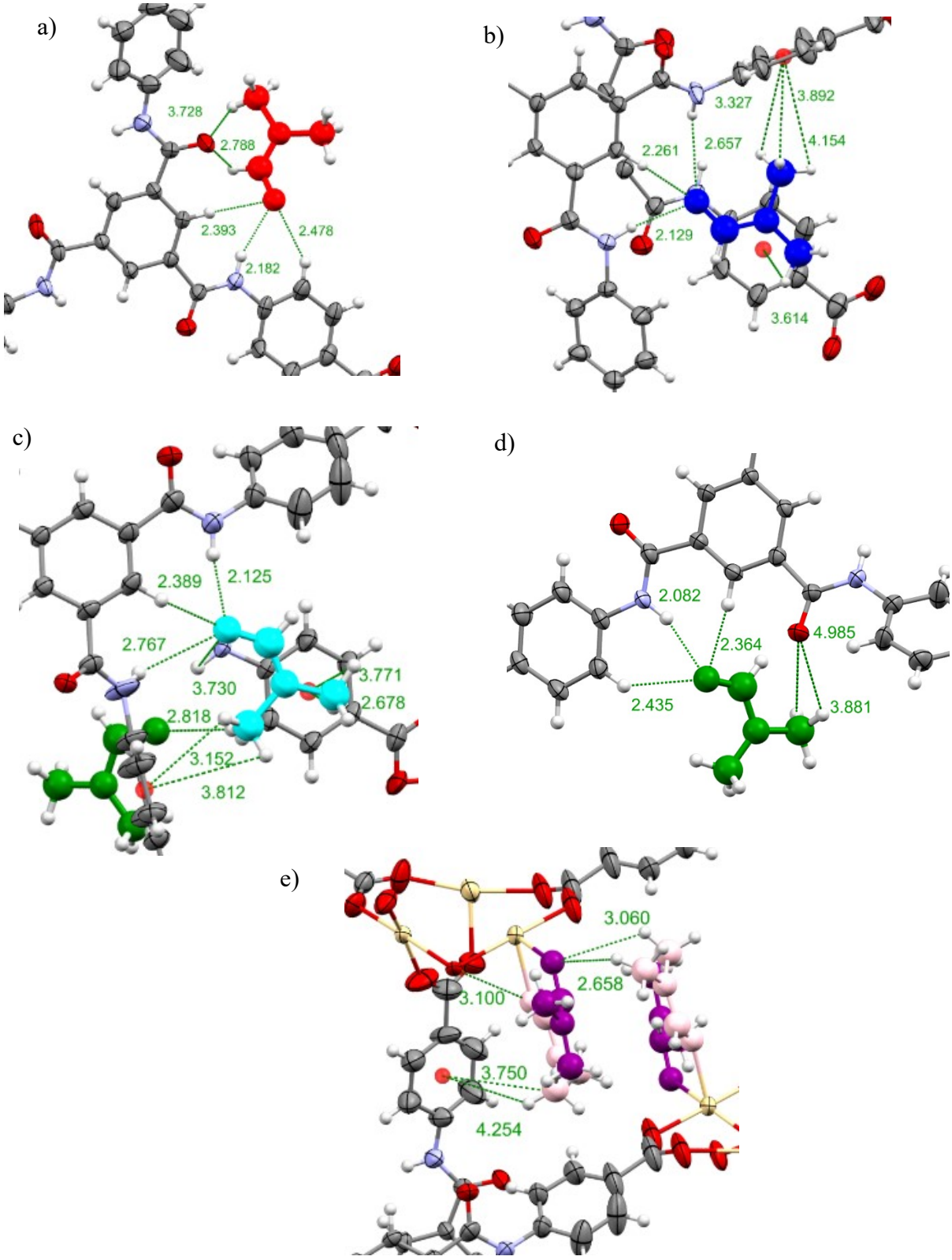

Figure S 2 Intermolecular interactions between DMF molecules shown in a) red, b) blue, c) turquoise, d) green and e) pink and the host framework ***2****. Interaction distances are displayed in angstroms.*

ii) Intermolecular interaction between acetonitrile molecules in the pore and sponge 2

Figure S3 a and b illustrates interactions between acetonitrile molecules shown in turquoise and pink with the framework. Both the molecules were bonded with the framework mainly by the hydrogen bonds. However, extra stabilisation of the molecule was obtained by additional CH-π interactions to hold the acetonitrile molecules in these particular sites.

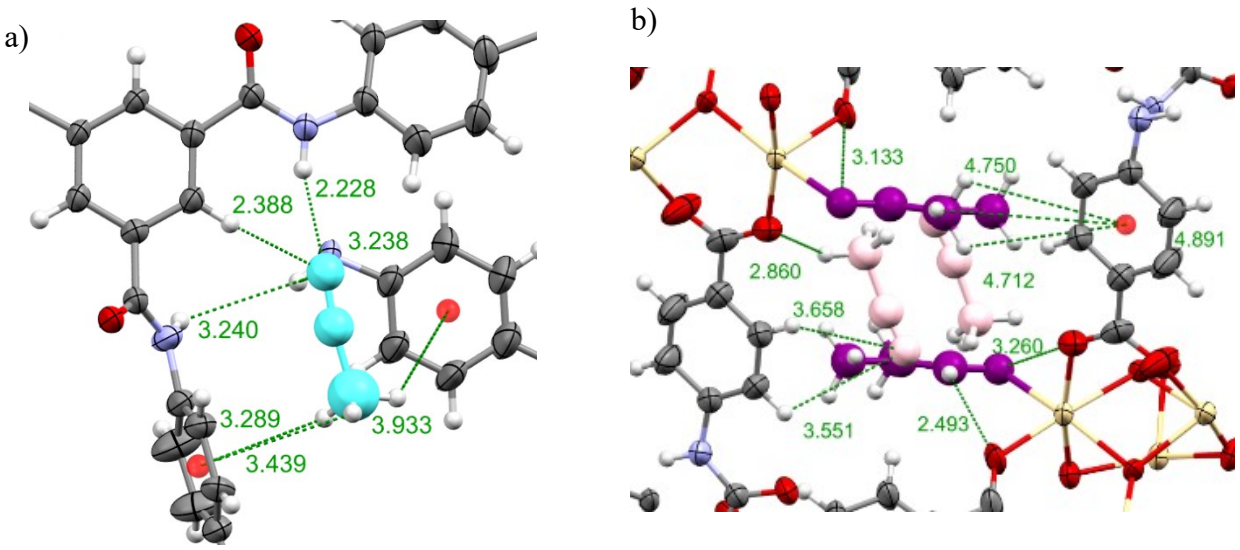

Figure S 3. a) Intermolecular interaction between turquoise acetonitrile and the host framework b) Intermolecular interaction between pink acetonitrile and the host framework. Acetonitrile molecules were displayed in ball stick. Interaction distances are displayed in angstroms.

iii) Intermolecular interaction between acetone molecules in the pore and sponge 2

Figure S4 a, b and c shows the interaction between acetone molecules in the pore and framework. The acetone molecules shown in lilac, light green, and orange occupied unique positions which was not observed in **2** or **2A**. The light green molecule of acetone is hydrogen-bonded with the framework of 2.3 Å and via CH-π with the framework of 3.8Å, as shown in Figure S4b. The acetone molecule shown in lilac and orange molecules are not involved in the hydrogen bonding because of they were isolated in the pore.

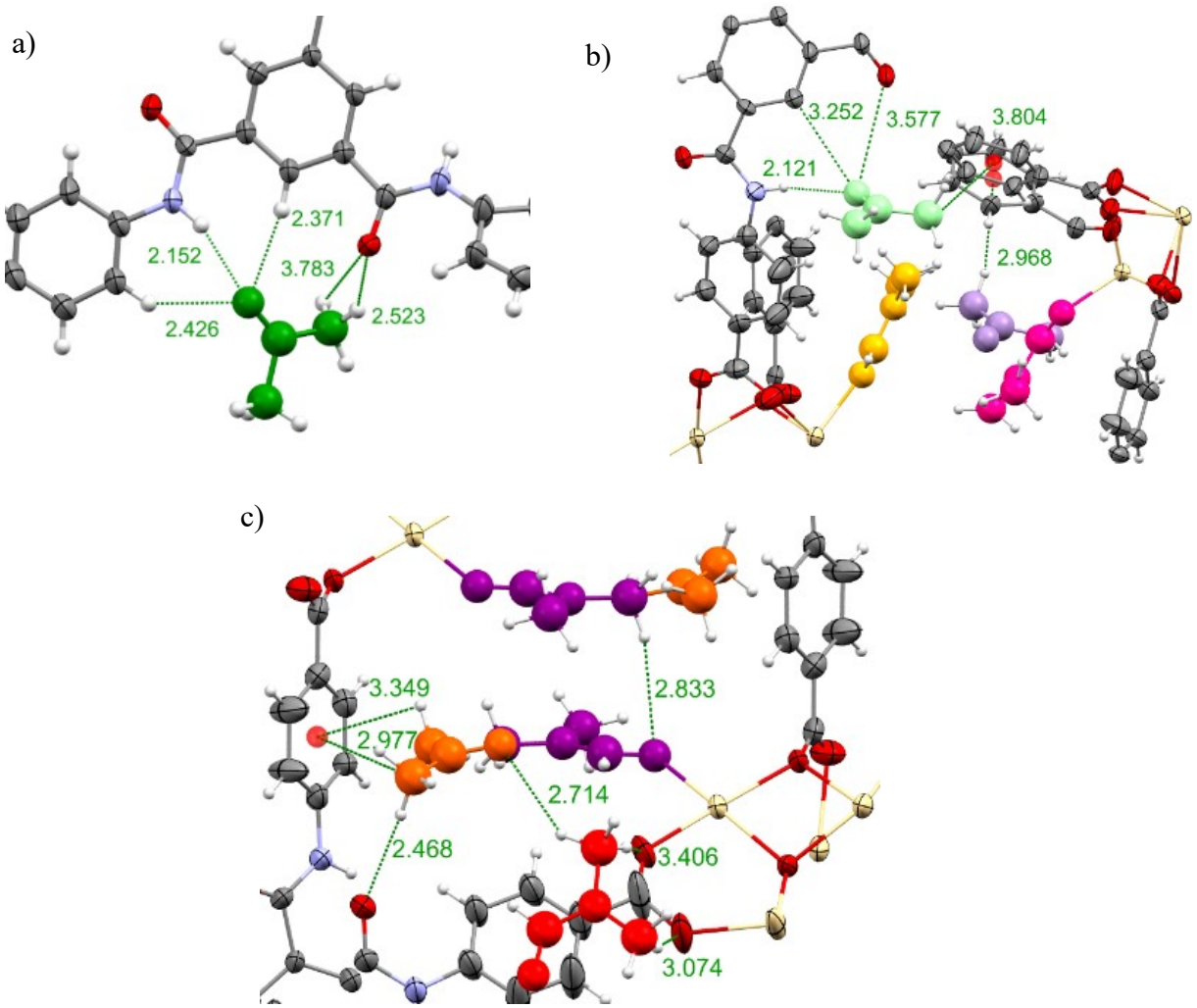

Figure S 4. Intermolecular interactions between acetone a) green b) light green and lilac c) orange with the host framework. Acetone molecules were displayed as ball stick models. Interaction distances are displayed in angstroms.

iv) Intermolecular interaction between isopropanol molecules in the pore and sponge 2

Six isopropanol molecules were observed in the pores. Figure S5a shows that the pink molecule is interacting with the framework via a hydrogen bond. Molecules of **C** identified in light green and orange occupied the same position common to both **2B** and **2C**, as shown in Figures S4c and S5b. In addition, a few unique positions were occupied by isopropanol molecules, as coloured in olive, light blue and cyan. The hydroxyl groups of the olive and light blue coloured **C** molecule forms a hydrogen bond with the carboxylates of the framework. Due to the proximity of the light blue molecule of **C** with the framework, a few CH-π were also observed. In contrast, the olive and cyan molecules are isolated in the pore thus no interaction with the framework was observed.

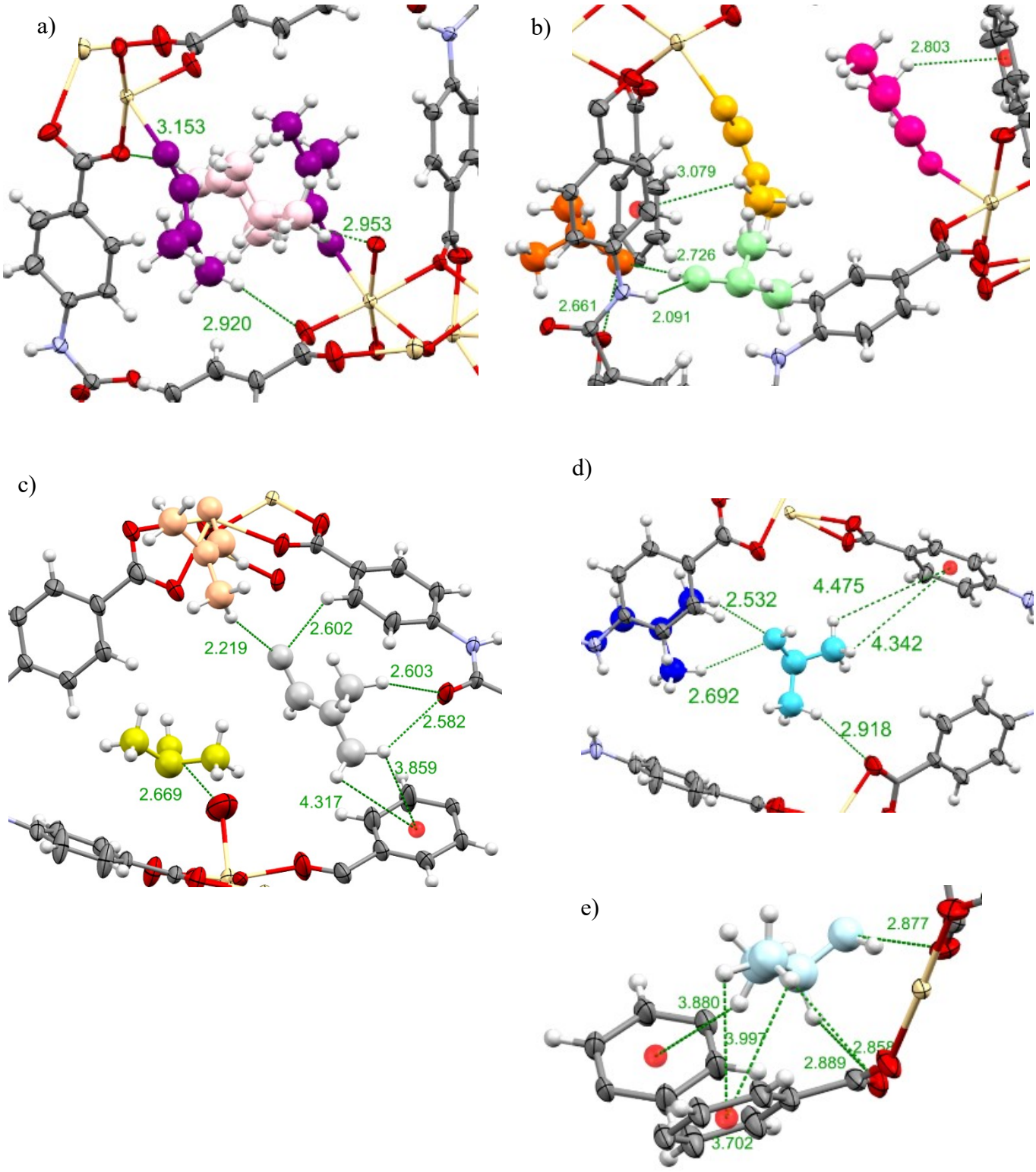

Figure S 5 Intermolecular interactions between isopropanol a) pink b) light green and orange c) olive d) cyan e) light blue and host framework. Guest molecules were displayed as ball and stick model. Interaction distances are displayed in angstroms.

S5. Optimisation of Encapsulation Conditions of Guests D and E in sponge 2

Guest 3,5-lutidine (**D**) is liquid at room temperature, therefore, soaking experiments with neat guest at 25 °C were performed to obtain high occupancies. The crystals of **2** remained stable in neat 3,5-lutidine. Guest 4-aminopyridine (**E**) is solid at room temperature therefore dissolved in acetone before soaking. The saturated solution resulted in quick deterioration of the crystals and hence several dilution conditions for soaking were attempted to obtain inclusion complex. Acetone was chosen for dilution of guests because crystals of **2** are stable in acetone and this solvent does not coordinate to the Cd^{2+} ions. In addition, dilution with acetone resulted in the successful replacement of DMF from all the coordination sites subsequently occupied by pyridine. Details of the soaking experiments and nature of crystals deterioration are given in Table S2

*Table S 2. Soaking conditions of 3,5-lutidine (**D**) and 4-aminopyridine (**E**) in sponge **2**.*

Guest	Concentration	Incubation period	Temperature	Results
3,5-lutidine (**D**)	neat	11 days	25 °C	7 guest molecules were observed bonded to Cd ions and 1 molecule in the pore
4-aminopyridine (**E**)	Saturated solution in acetone	1 day	25 °C	Several cracks developed in the crystals and were not diffracting.
4-aminopyridine (**E**)	0.02 g in 2 mL acetone	8 days	25 °C	2 guest molecules were observed bonded to Cd ions
4-aminopyridine (**E**)	0.05 g in 2 mL acetone	1 week	25 °C	8 guest molecules were observed bonded to Cd ions

S6. Optimisation of Encapsulation Conditions of Guests F and G sponge 2 and 3

Guest molecules *N*,*N*-dimethylaniline and propiophenone are liquid at room temperature. Therefore, neat guests were used for soaking crystals of **2** to obtain inclusion complexes **2F** and **2G**. Soaking of crystals of **2** with diluted guests were also attempted however, guest molecules were not observed in the pores. To obtain inclusion complexes **3F** and **3G**, crystals of **3** were first soaked in neat guests, however, deterioration of the crystals were observed. Therefore, guests were diluted with acetone prior to soaking. Details of soaking experiments and nature of crystal deterioration are given in Table S3

*Table S 3 Soaking condition of N,N dimethylaniline and propiophenone in sponge **2** and **3**.*

Guest	Sponge	Guest dilution conditions	Solvent (1ml)	Incubation period	Results
N,*N*-dimethylaniline (**F**)	**2**	neat	-	1 week	2 guest molecules in the pore (**2F**)
N,*N*-dimethylaniline (**F**)	**2**	neat	-	2 weeks	Crystals look fine optically but do not diffract
N,*N*-dimethylaniline (**F**)	**2**	100 μL	DMF	3 days	No guest was observed in the pore
N,*N*-dimethylaniline (**F**)	**2**	50 μL	DMF	3 days	No guest was observed in the pore
N,*N*-dimethylaniline (**F**)	**3**	neat	-	1 day	Crystal deteriorated
N,*N*-dimethylaniline (**F**)	**3**	50 μL	Acetone	3 days	1 guest molecule in the pore (**3F**)
N,*N*-dimethylaniline (**F**)	**3**	50 μL	Acetone	1 week	Crystals look fine optically but do not diffract
N,*N*-dimethylaniline (**F**)	**3**	100 μL	Acetone	3 days	1 disordered guest molecule in the pore
Propiophenone (**G**)	**2**	neat	-	1 day	4 guest molecules in the pore (**2G**)
Propiophenone (**G**)	**2**	100 μL	DMF	10 days	No guest was observed in the pore
Propiophenone (**G**)	**3**	neat	-	1 day	Crystals deteriorated
Propiophenone (**G**)	**3**	100 μL	Acetone	10 days	1 guest molecule in the pore (**3G**)
Propiophenone (**G**)	**3**	500 μL	Acetone	10 days	1 guest molecule in the pore

S7. Geometry of Cd1-Cd7 ions in sponge 3 parallel to that used in S1

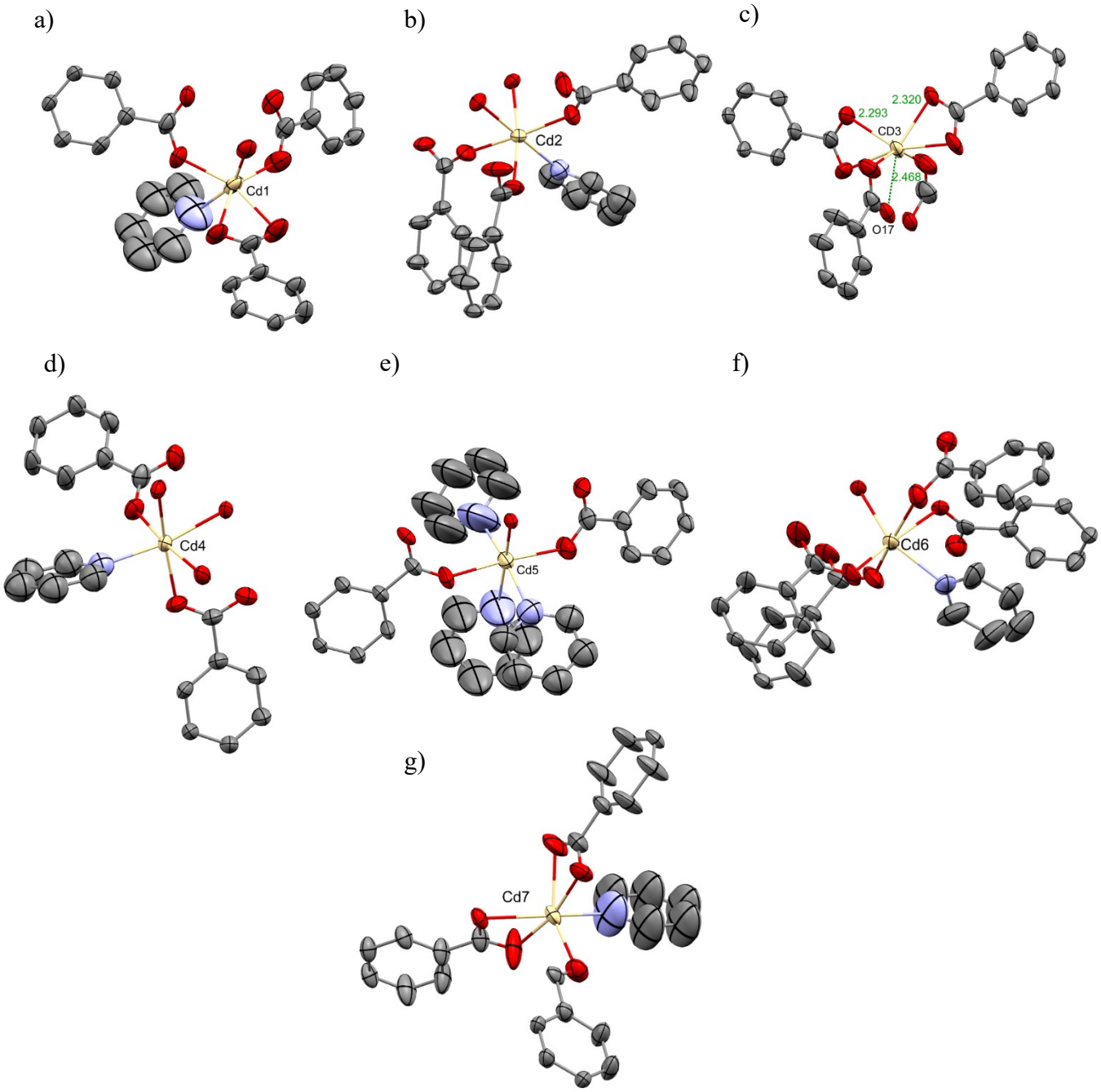

Figure S 6 a)-g) Geometry of Cd1-Cd7 ions surrounded by linker molecules, μ3-O ligands, water molecules and pyridine molecules. Framework displayed in ellipsoids at 50% probability.

S8. General crystallographic refinement details

Unit cell determination, data reduction, and absorption corrections were carried out using CrysAlisPro.[1] The structures were solved by direct methods and refined by full-matrix least-squares based on F^2 using SHELXL[2] within the OLEX 2.0[3] graphical user interface. The non-hydrogen atoms of the framework were refined anisotropically and hydrogen atoms were included using a riding model. All the molecules either bonded to Cd or guests found in the pore were first fully identified by the electron density map and initially refined without constraints but due to problems with convergence restraints/constraints were applied as reported in the final structures. Restrains/constrains were used to resolve the disorders in the structure and to obtain stable model. For example, the BTA and Cd components of the framework were at first freely refined without applying any constraints/restraints. However, on rare occasions the BTA, Cd and coordinated DMF components of the framework showed some disorder and where required atoms were modelled across two positions with a combined occupancy of 100% were used. DFIX, ISOR and EADP were used to obtain a stable model. Similarly, the chemical structure of solvent species were first unambiguously identified and then refinement was first performed without any constraints/restraints and only if this was unsuccessful, were these added based on their known structures. The occupancy of each solvent molecule was refined against its free variable which in the final stages of refinement was fixed to values reported. In addition, some disorders were observed in the DMF molecules (coordinated and in the pores) and the guest solvent molecules in the pores were modelled across two positions with a combined occupancy of 100% were used. All the guest molecules were refined anisotropically and where necessary DFIX was applied to achieve acceptable geometry and a stable model. ISOR and EADP were applied to restrain the ADPs. In all structures hydrogen atoms were added by the riding model. However, for some molecules hydrogens were required to be placed in fixed positions. In all the structures it was not possible to

assign all the residual density peaks in a way that makes chemical sense, these peaks belong to heavily disordered guests or solvent molecules, and these were taken into account by the use of the SQUEEZE function within the PLATON. On occasion a large residual density peak remained near the cadmium metal of the host framework this is due to absorption and/or termination errors in Fourier calculation. Details of the refinement of the guests molecules were given in the section below. Similar to the solvent species, the chemical structure of the guest molecules were unambiguously identified by the electron density maps and then refinement was first performed without any constraints/restraints and only if this was unsuccessful, were these added based on the known structures of the guest species.

S9. Refinements details of individual inclusion complex

Sponge 2

CSD Deposition Number 2243754

The asymmetric unit of four consists of four BTA^{3-} linkers, seven Cd^{2+} ions, four coordinated DMF molecules and six DMF molecules in the pore. Anisotropic refinement of the non-hydrogen atoms of sponge **2** was performed by applying constraints/restraints to achieve a stable model. ISOR and EADP was used to constrain the atomic displacement parameters of the coordinated DMF molecules to similar values. DFIX and SIMU were used to fix bond lengths of DMF molecules in the pores to obtain a realistic and acceptable geometry. The solvent mask detected one significant void 71104 $Å^3$ in size containing 1584 electrons. A large residual peak (5.4 e/Å) was found closer to Cd ion, this is due absorption.

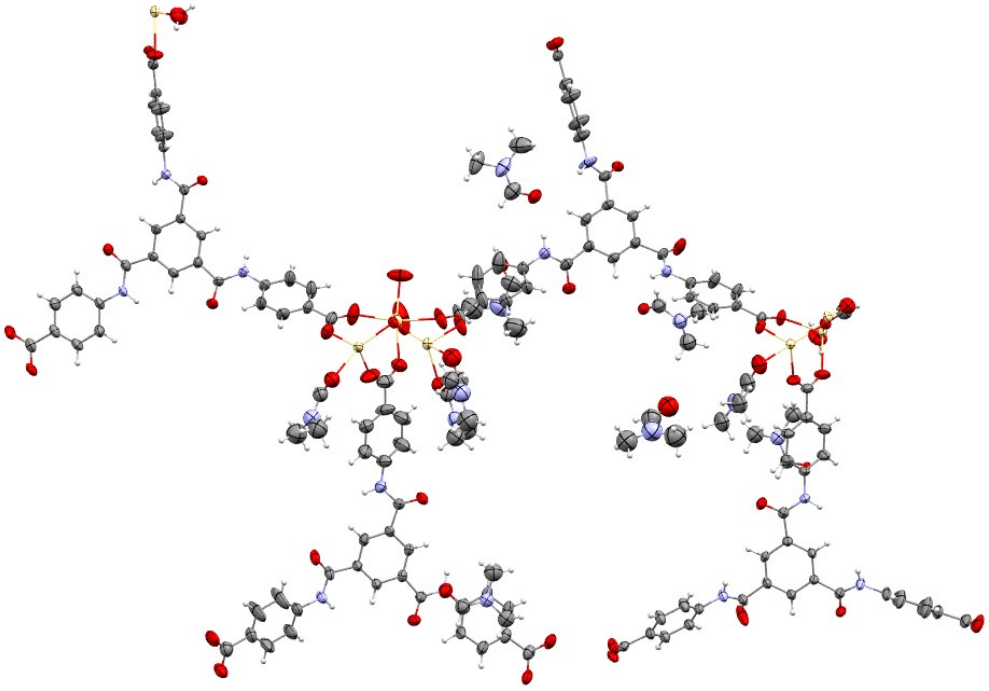

*Figure S 7. Asymmetric unit of sponge **2**.*

Inclusion complex 2A

CSD Deposition Number 2243755

The asymmetric unit of **2A** four consists of four BTA^{3-} linkers, seven Cd^{2+} ions, four coordinated DMF molecules, two DMF molecules in the pore and two acetonitrile molecules in the pore. BTA linker and coordinated DMF shows disorder and refined across two positions with combined occupancy of 100%. Acetonitrile molecules were refined anisotropically and where necessary DFIX was applied to achieve acceptable geometry and a stable model. ISOR and EADP were applied to restrain the ADPs. The solvent mask detected one significant void 6864 $Å^3$ in size containing 1510 electrons. A large residual peak (4.5 e/ Å) was found closer to O20, this peak could not be assigned in a way that makes any chemical sense.

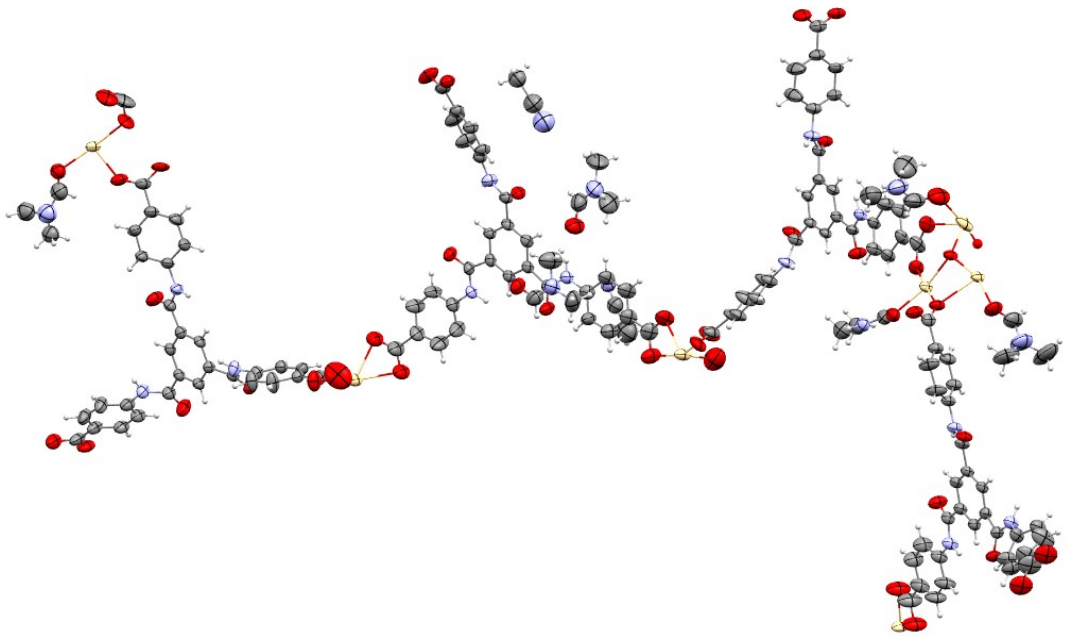

*Figure S 8. Asymmetric unit of inclusion complex **2A**, showing major components of disorder only.*

Inclusion complex 2B

CSD Deposition Number 2243756

The asymmetric unit of **2B** four consists of four BTA^{3-} linkers, seven Cd^{2+} ions, three coordinated DMF molecules, three DMF molecules in the pore and four acetone molecules in the pore. O14 and Cd5 shows disorder and therefore refined across two positions with combined occupancy of 100%. Acetone molecules were refined with 100% occupancy. The solvent mask detected one significant void 6257 $Å^3$ in size containing 1435 electrons. A large residual peak (3.9 e/Å) was found closer to Cd ion, this is due absorption and/or termination errors in the Fourier calculations.

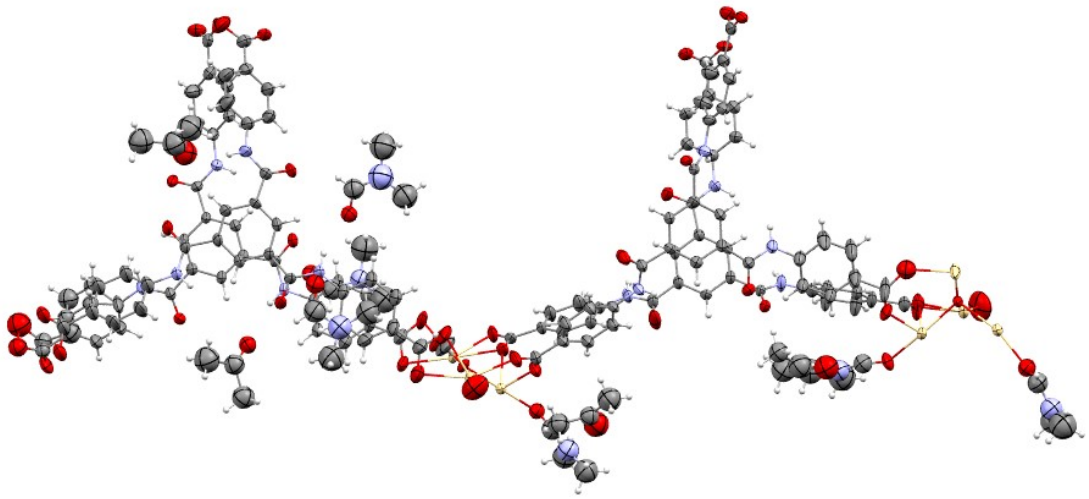

*Figure S 9. Asymmetric unit of inclusion complex **2B**, showing major components of disorder only.*

Inclusion complex 2C

CSD Deposition Number 2243760

The asymmetric unit of **2C** four consists of four BTA^{3-} linkers, seven Cd^{2+} ions, five coordinated DMF molecules, five DMF molecules in the pore and six isopropanol molecules in the pore. Isopropanol molecules found in the pores were refined anisotropically and where necessary DFIX, ISOR and EADP were applied to achieve a stable model. The solvent mask detected two significant voids 769 $Å^3$ and 472 $Å^3$ in size containing 188 and 127 electrons respectively. A large residual peak (9.8 e/Å) was found closer to Cd ion, this is due absorption and/or termination errors in the Fourier calculations.

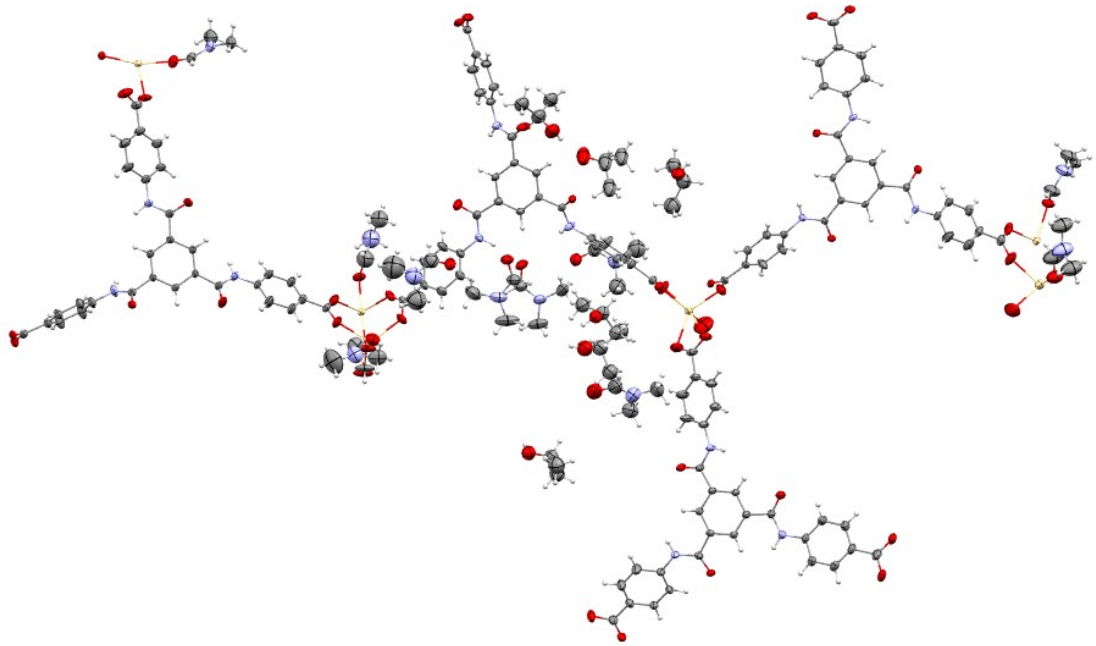

*Figure S 10. Asymmetric unit of inclusion complex **2C**.*

Inclusion complex 3

CSD Deposition Number 2240137

The asymmetric unit of **3**, four consists of four BTA^{3-} linkers, seven Cd^{2+} ions, and seven coordinated pyridine molecules. In the pore two DMF molecules, three acetone molecules and one pyridine molecule were observed. In this complex pyridine molecules are part of the framework. Disordered pyridine molecules were observed and where necessary atoms were modelled over the two positions with combined occupancies of 100%. DFIX was applied to fix the bond lengths, and AFIX was used to make the pyridine ring rigid. On several pyridine molecules EADP and ISOR were used to constrain the atomic displacement parameter to similar values. The solvent mask detected two significant voids 1662 $Å^3$ and 355 $Å^3$ in size containing 406 and 71 electrons respectively. A large residual peak (2.6 e/Å) was found closer to N11, this peak could not be assigned in a way that makes any chemical sense.

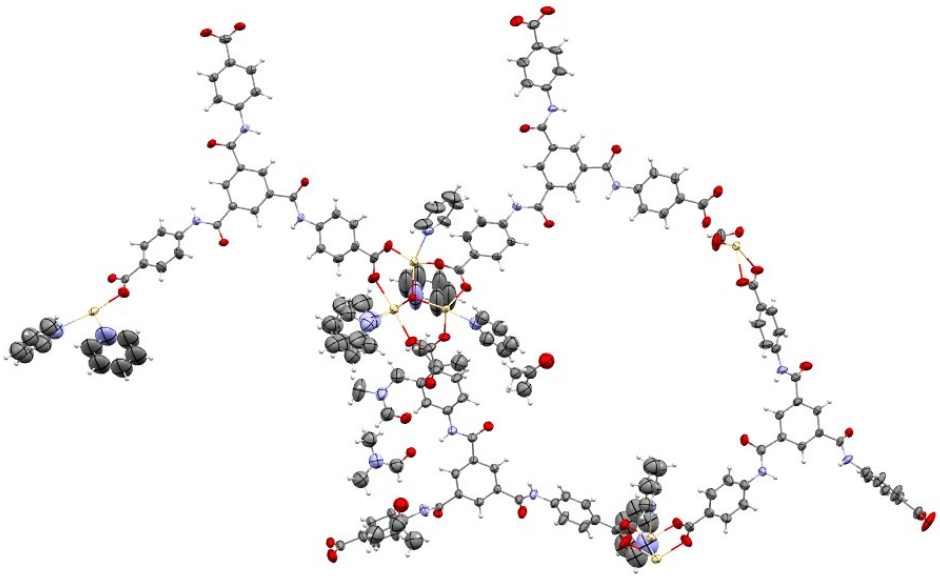

*Figure S 11. Asymmetric unit of inclusion complex **3**, showing major components of disorder only.*

Inclusion complex 2D

CSD Deposition Number 2243761

The asymmetric unit of **2D** consists of four BTA^{3-} linkers and seven Cd^{2+} ions. Seven guest molecules bonded to Cd ions. One guest molecule was in the pore along with three DMF molecules. All non-hydrogen atoms of 3,5-lutidine molecules bonded to Cd^{2+} and in the pore were refined anisotropically by applying DFIX, AFIX and EADP where necessary, to achieve acceptable geometry and a stable model. Disorder in components of BTA linker and in few molecules of 3,5-lutidine were observed and atoms were modelled over the two positions with combined occupancies of 100% (Figure S13). The solvent mask detected one significant void 2220 $Å^3$ in size containing 505 electrons. A large residual density peak (7.3 e/Å) was observed closer to Cd ion, this is due to absorption and/or termination error in Fourier calculations.

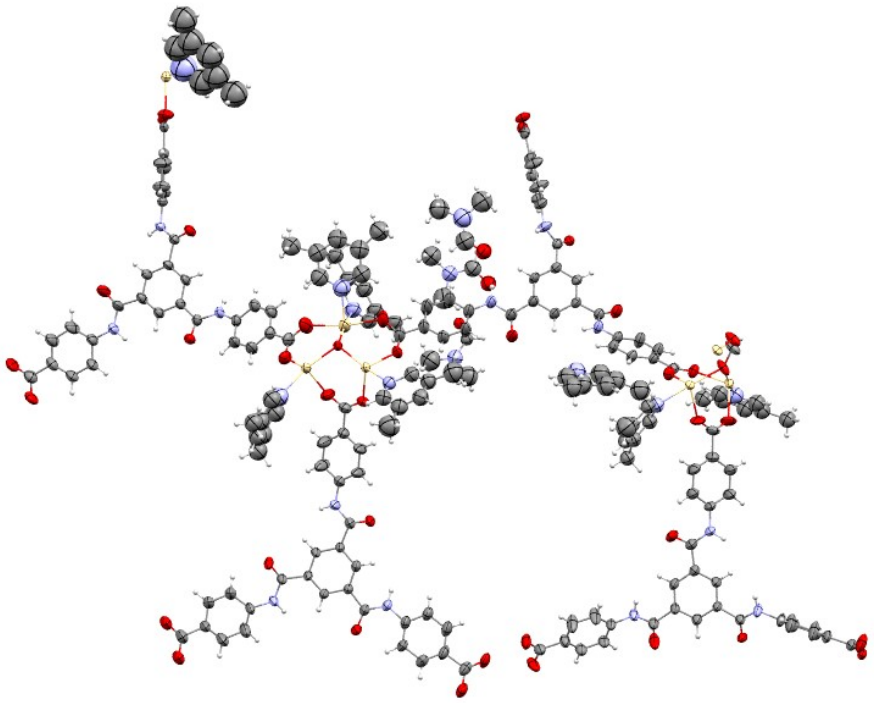

*Figure S 12. Asymmetric unit of inclusion complex **2D**, showing major components of disorder only.*

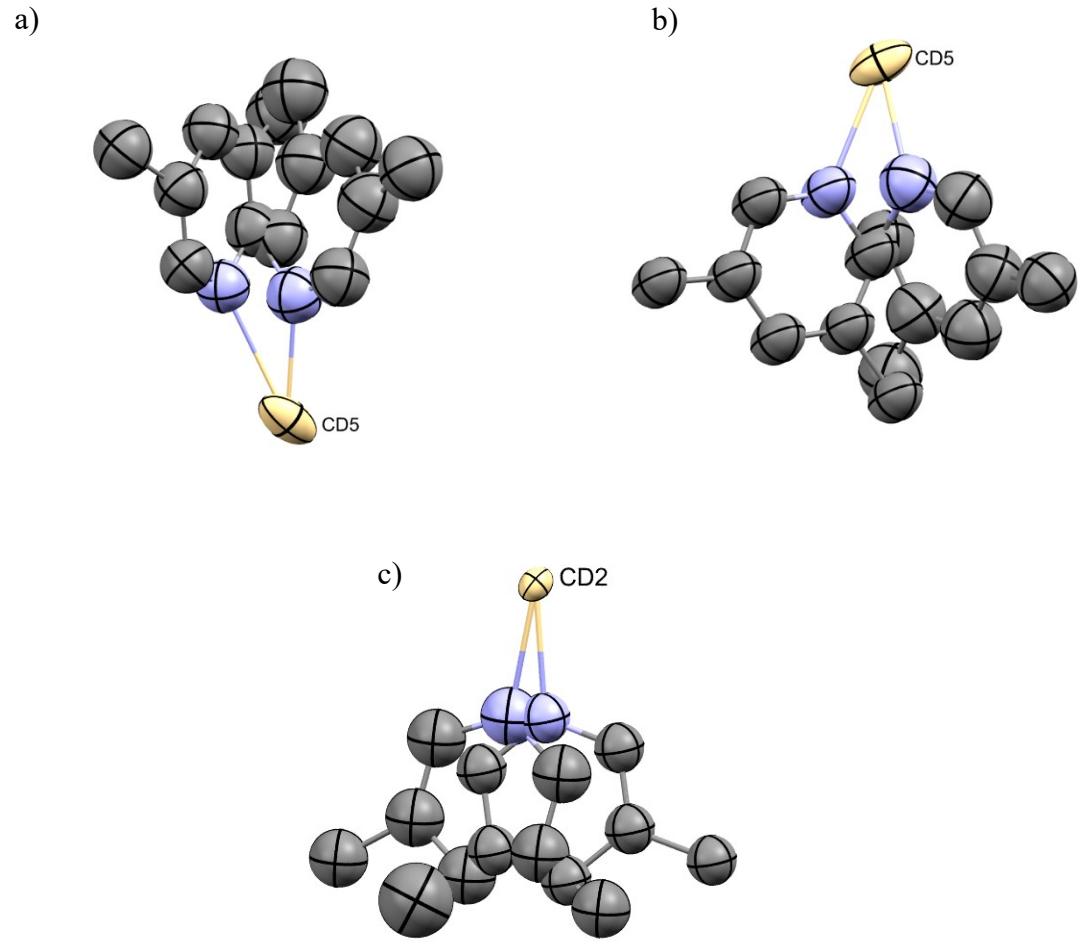

Figure S 13 a) and b) Disorder in the molecules of 3,5 lutidine bonded to Cd5. c) Disorder in the molecules of 3,5 lutidine bonded to Cd5. Guest molecule is shown in ellipsoids with 50% probability

Inclusion complex 2E

CSD Deposition Number 2243762

The asymmetric unit of **2E** consists of four BTA^{3-} linkers and seven Cd^{2+} ions. Eight guest molecules bonded to Cd ions. One DMF molecule and three acetone molecules are in the pore. 4-aminopyridine molecule bonded to Cd4 shows disorder and therefore the atoms were refined across two positions with combined occupancy of 100% as shown in Figure S15. DFIX, AFIX, ISOR and EADP were applied to 4-aminopyridine molecules to achieve acceptable geometry and a stable mode. The solvent mask detected one significant void 5883 $Å^3$ in size containing 1072 electrons.

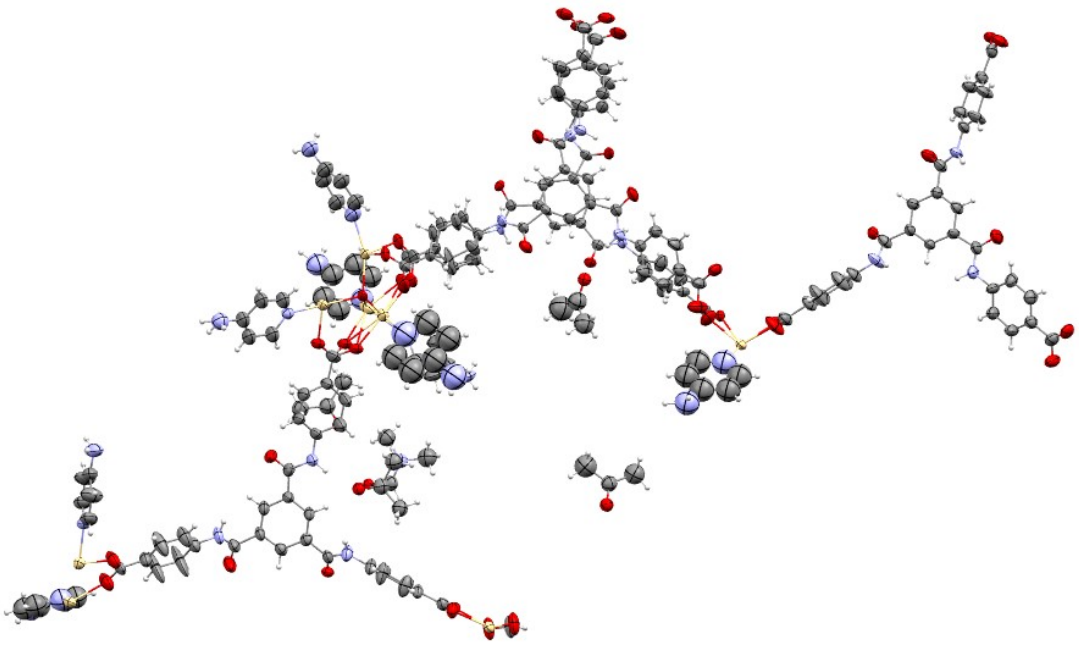

*Figure S 14. Asymmetric unit of inclusion complex **2E**, showing major components of disorder only.*

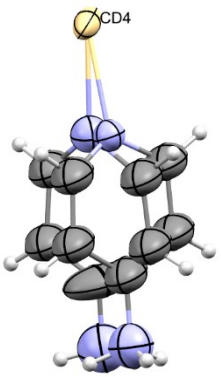

Inclusion complex 2F

CSD Deposition Number 2243758

The asymmetric unit of **2F** consists of four BTA^{3-} linkers, seven Cd^{2+} ions, two molecules of DMF bonded to Cd^{2+} ions and four molecules of DMF in the pore together with two molecules of *N*,*N*-dimethylaniline in the pores. Non-hydrogen atoms of both the molecule were refined anisotropically and DFIX, AFIX and EADP were applied to the molecule to achieve acceptable geometry. Cd7 shows disorder and therefore refined across two positions with combined occupancy of 100%. The solvent mask detected one significant void 3770 $Å^3$ in size containing 735 electrons respectively. A large residual density peak (3.8 e/Å) was observed closer to Cd ion, this is due to absorption and/or termination error in Fourier calculations.

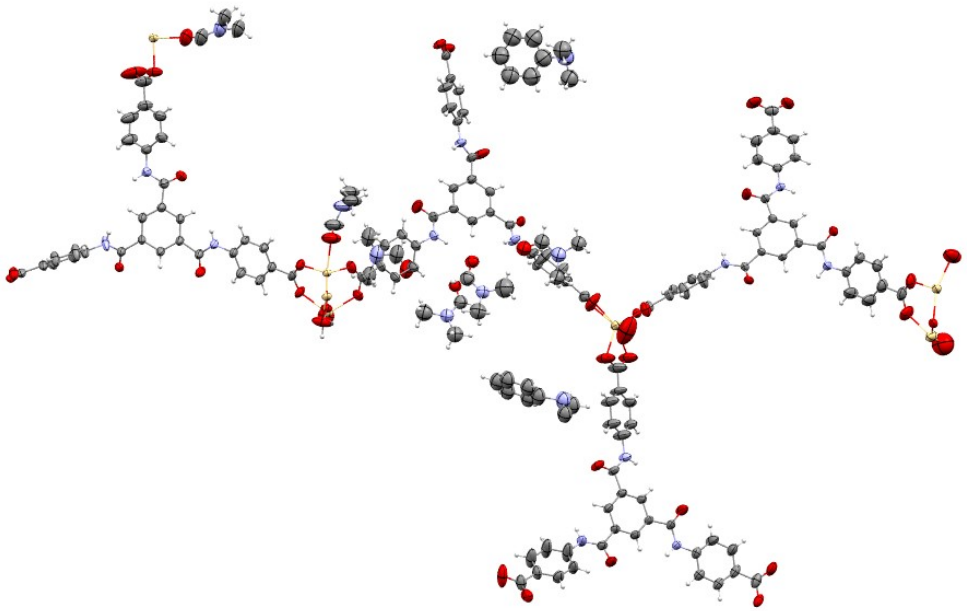

*Figure S 16. Asymmetric unit of inclusion complex **2F**, showing major components of disorder only.*

Inclusion complex 3F

CSD Deposition Number 2243757

The asymmetric unit of **3F** consists of four BTA^{3-} linkers, seven Cd^{2+} ions and seven pyridine ligands bonded to Cd^{2+} ions, and one molecule of *N*,*N*-dimethylaniline and seven molecules of acetone in the pores. One of the pyridine rings show disorder and the atoms were refined across two position with combined occupancy of 100%. The *N*,*N*-dimethylaniline molecule was refined anisotropically with DFIX and AFIX applied to the molecule to achieve acceptable geometry. Seven acetone molecules refined in the pores were anisotropically refined. DFIX and EADP were applied on acetone molecules where necessary. The solvent mask detected three significant voids 598 $Å^3$, 443 $Å^3$ and 289 $Å^3$ in size containing 102, 103 and 64 electrons respectively. A large residual density peak (5.1 e/Å) was observed closer to N10, this peak could not be assigned in a way that makes any chemical sense.

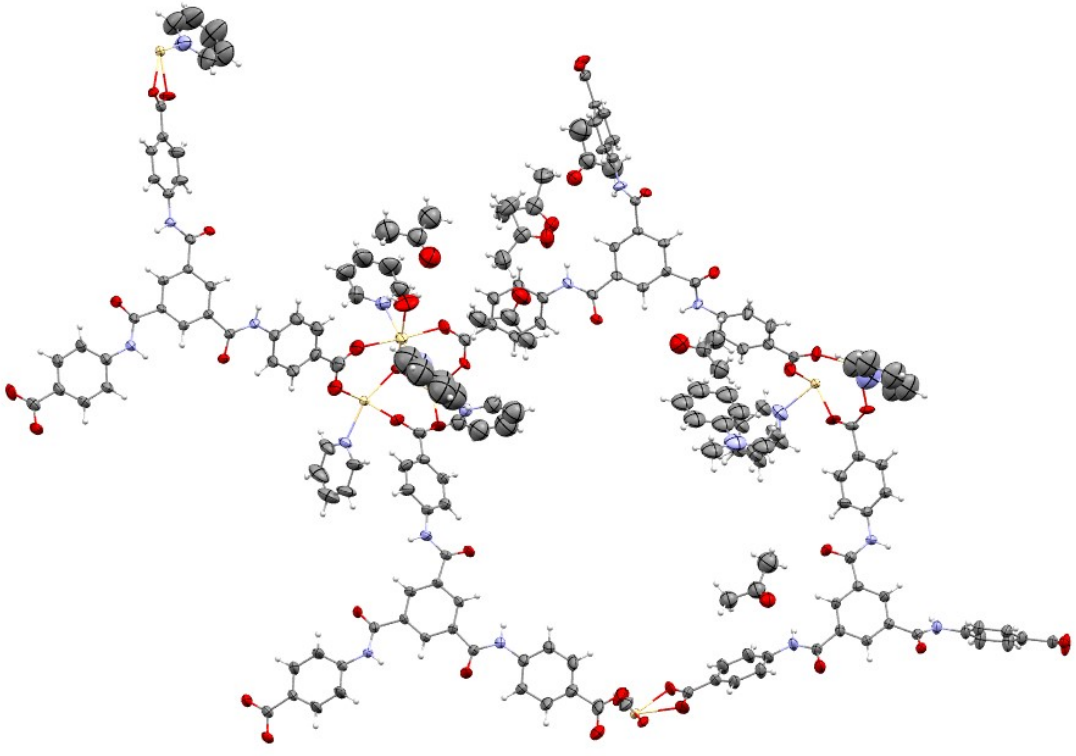

*Figure S 17. Asymmetric unit of inclusion complex **3F**, showing major components of disorder only.*

Inclusion complex 2G

CSD Deposition Number 2243759

The asymmetric unit of **2G** consists of four BTA^{3-} linkers, seven Cd^{2+} ions, four molecules of DMF bonded to Cd^{2+} ions and three DMF molecules in the pore together with four molecules of propiophenone in the pores. BTA and Cd component of the framework shows disorder and refined across two positions with combined occupancy of 100 %. Four molecules of propiophenone were refined anisotropically. DFIX, AFIX and EADP were applied to the propiophenone molecules to achieve acceptable geometry and a stable mode. The solvent mask detected one significant void 2395 $Å^3$ in size containing 640 electrons. A large residual density peak (2.4 e/Å) was observed closer to Cd ion, this is due to absorption and termination error in Fourier calculations.

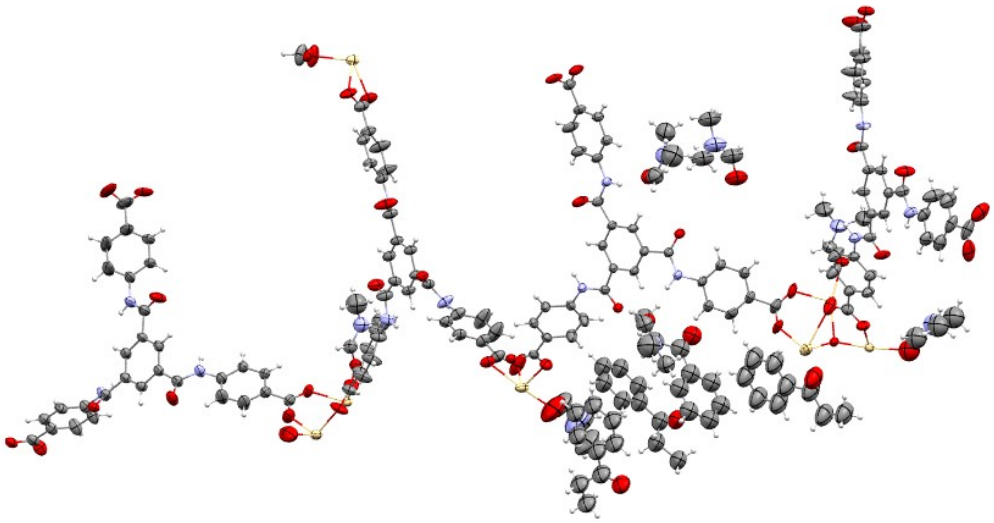

*Figure S 18. Asymmetric unit of inclusion complex **2G**, showing major components of disorder only.*

Inclusion complex 3G

CSD Deposition Number 2240138

The asymmetric unit of **3G** consists of four BTA^{3-} linkers, seven Cd^{2+} ions, and seven molecules of pyridine bonded to Cd^{2+} ions and four acetone molecules in the pore together with one molecule of propiophenone in the pore. Propiophenone molecule was refined anisotropically with 50% occupancy and DFIX, AFIX and EADP were applied to this molecule to achieve acceptable geometry. Acetone molecules in the pore were refined anisotropically and constrain/restrain applied where necessary. The solvent mask detected one significant void 5221 $Å^3$ in size containing 1204 electrons. A large residual density peak (2.6 e/Å) was observed closer to Cd ion, this is due to absorption and termination error in Fourier calculations.

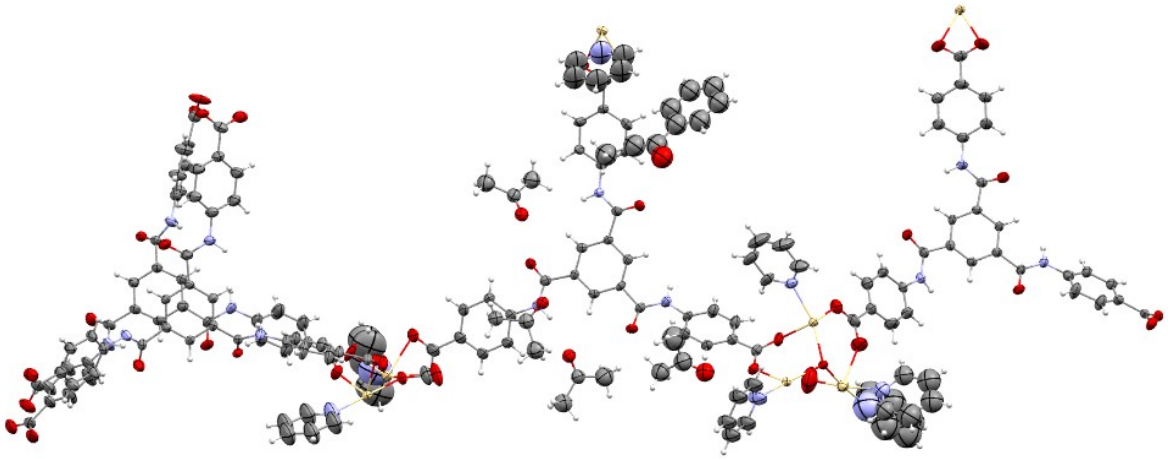

*Figure S 19. Asymmetric unit of inclusion complex **3G**.*

S10. Crystallographic Tables

*Table S 4. Crystallographic table of inclusion complexes **2**, **2A**, **2B**, **2C** and **3**.*

Inclusion complexes	**2**	**2A**	**2B**	**2C**	**3**
Empirical formula	$C_{148\cdot5}H_{135.5}Cd_7N_{21}O_{52}$	$C_{142.2}H_{124.2}Cd_7N_{19.5}O_{47}$	$C_{142.23}H_{121.47}Cd_7N_{17}O_{47.32}$	$C_{159.73}H_{162.49}Cd_7N_{21.75}O_{54}$	$C_{168.79}H_{137.80}Cd_7N_{21}O_{42.88}$
Formula weight	3833.07	3645.00	2890.27	2691.77	2621.86
Temperature/K	150(1)	150(1)	150(1)	150(1)	150(1)
Crystal system	monoclinic	monoclinic	monoclinic	monoclinic	monoclinic
Space group	$P2_1/n$	$P2_1/n$	$P2_1/n$	$P2_1/n$	$P2_1/n$
a/Å	14.6954(2)	13.6817(2)	13.9475(2)	14.52210(10)	14.02999(14)
b/Å	42.2913(4)	43.2808(4)	43.3134(4)	42.7754(2)	43.3663(3)
c/Å	33.8929(4)	33.7646(4)	33.5321(4)	33.9548(2)	33.7009(2)
α/°	90	90	90	90	90
β/°	91.6490(10)	95.3182(14)	94.4569(11)	93.4290(10)	94.3810(8)
γ/°	90	90	90	90	90
V/Å^3	21055.3(4)	19907.9(5)	20195.9(4)	21054.6(2)	20444.7(3)
Z	4	4	4	4	4
ρ_{calc}g/cm^3	1.61	1.212	1.224	1.273	1.307
μ/mm^{-1}	6.143	6.289	6.376	6.177	6.322
F(000)	7128	7269	7466	8156	8096
Crystal size/mm^3	0.28 × 0.13 × 0.06	0.24 × 0.12 × 0.08	0.27 × 0.15 × 0.06	0.25 × 0.15 × 0.05	0.24 × 0.13 × 0.06
Radiation	CuK_α (λ = 1.54184)	CuK_α (λ = 1.54184)	CuK_α (λ = 1.54184)	CuK_α (λ = 1.54184)	CuK_α (λ = 1.54184)
2Θ range for data collection/°	6.818 to 145.824	7.074 to 146.946	6.996 to 147.07	7.082 to 147.072	6.656 to 147.438
Index ranges	−18 ≤ h ≤ 12, −52 ≤ k ≤ 49,−41 ≤ l ≤ 40	−16 ≤ h ≤ 16, −38 ≤ k ≤ 53, −41 ≤ l ≤ 28	−17 ≤ h ≤ 15, −51 ≤ k ≤ 53, −41 ≤ l ≤ 40	−17 ≤ h ≤ 16, −52 ≤ k ≤ 52, −39 ≤ l ≤ 42	−17 ≤ h ≤ 17, −53 ≤ k ≤ 53, −41 ≤ l ≤ 41
Reflections collected	160787	81548	148527	166701	378169
Independent reflections	41170 [R_{int} = 0.0586, R_{sigma} = 0.0457]	38920 [R_{int} = 0.0478, R_{sigma} = 0.0556]	40073 [R_{int} = 0.0671, R_{sigma} = 0.0513]	41795 [R_{int} = 0.0486, R_{sigma} = 0.0351]	40915 [R_{int} = 0.0836, R_{sigma} = 0.0315]
Data/restraints/parameters	41170/381/2066	38920/148/2052	40073/466/2091	41795/239/2221	40915/530/2102
Goodness-of-fit on F^2	1.017	1.077	1.021	1.040	1.042
Final R indexes [I>=2σ (I)]	R_1 = 0.0751, wR_2 = 0.2019	R_1 = 0.0757, wR_2 = 0.2108	R_1 = 0.0840, wR_2 = 0.2194	R_1 = 0.0686, wR_2 = 0.2034	R_1 = 0.0781, wR_2 = 0.2130
Final R indexes [all data]	R_1 = 0.0946, wR_2 = 0.2235	R_1 = 0.0906, wR_2 = 0.2280	R_1 = 0.1078, wR_2 = 0.2446	R_1 = 0.0737, $wR2$ = 0.2124	R_1 = 0.0877, $wR2$ = 0.2235
Largest diff. peak/hole / e Å^{-3}	5.45/−2.70	4.5/−1.91	3.29/−2.17	9.80/−3.38	2.59/−2.09

*Table S 5. Crystallographic table of inclusion complexes **2D** and **2E**.*

Inclusion complex	**2D**	**2E**
Empirical formula	$C_{178.65}H_{153.04}Cd_7N_{21.55}O_{41.29}$	$C_{155.65}H_{124.75}Cd_{6.9}N_{23.2}O_{42.15}$
Formula weight	2699.58	3770.09
Temperature/K	150(1)	150(1)
Crystal system	monoclinic	monoclinic
Space group	$P2_1/n$	$P2_1/n$
a/Å	14.75582(16)	14.9412(2)
b/Å	42.9510(3)	42.7238(4)
c/Å	33.8388(3)	33.8725(4)
α/°	90	90
β/°	93.4415(9)	93.6969(14)
γ/°	90	90
V/Å^3	21407.6(3)	21577.4(5)
Z	4	4
ρ_{calc}g/cm^3	1.287	1.192
μ/mm^{-1}	6.048	5.896
F(000)	8386	7770
Crystal size/mm^3	0.24 × 0.05 × 0.03	0.25 × 0.063 × 0.02
Radiation	Cu K_α (λ = 1.54184)	Cu K_α (λ = 1.54184)
2Θ range for data collection/°	7 to 146.954	6.948 to 147.034
Index ranges	$-15 \le h \le 18$, $-52 \le k \le 51$, $-39 \le l \le 41$	$-18 \le h \le 17$, $-53 \le k \le 44$, $-35 \le l \le 42$
Reflections collected	163450	170415
Independent reflections	42568 [R_{int} = 0.0486, R_{sigma} = 0.0357]	42835 [R_{int} = 0.0514, R_{sigma} = 0.0380]
Data/restraints/parameters	42568/965/2178	42835/424/2084
Goodness-of-fit on F^2	1.059	1.060
Final R indexes [$I>=2\sigma(I)$]	R_1 = 0.0921, wR_2 = 0.2367	R_1 = 0.1097, wR_2 = 0.2818
Final R indexes [all data]	R_1 = 0.1038, wR_2 = 0.2480	R_1 = 0.1177, wR_2 = 0.2881
Largest diff. peak/hole / e Å^{-3}	7.34/−1.82	1.92/−1.30

*Table S 6. Crystallographic table of inclusion complexes **2F**, **3F**, **2G** and **3G***

Inclusion complex	**2F**	**3F**	**2G**	**3G**
Empirical formula	$C_{148.3}H_{126}Cd_7N_{18.85}O_{49}$	$C_{172.5}H_{145.33}Cd_7N_{19}O_{45.83}$	$C_{168.19}H_{147.50}Cd_7N_{18.49}O_{49.54}$	$C_{168}H_{127.99}Cd_7N_{19}O_{44.50}$
Formula weight	2945.91	4004.52	2284.01	2606.78
Temperature/K	150(1)	150(1)	150(1)	150(1)
Crystal system	monoclinic	monoclinic	monoclinic	monoclinic
Space group	$P2_1/n$	$P2_1/n$	$P2_1/n$	$P2_1/n$
a/Å	14.6869(11)	14.1427(3)	14.61500(10)	14.05890(12)
b/Å	42.8432(3)	43.1990(6)	43.0674(3)	43.1549(2)
c/Å	33.8507(2)	33.7991(4)	33.6023(2)	33.7222(2)
α/°	90	90	90	90
β/°	93.1111(7)	94.7053(16)	93.6760(10)	94.5246(7)
γ/°	90	90	90	90
V/Å^3	21268.7(3)	20580.0(6)	21106.8(2)	20395.9(2)
Z	4	4	4	4
ρ_{calc}g/cm^3	1.150	1.299	1.260	1.256
μ/mm^{-1}	6.049	6.288	6.140	6.312
F(000)	7371	8104	8060	7724
Crystal size/mm^3	0.25 × 0.05 × 0.01	0.23 × 0.05 × 0.04	0.15× 0.08 × 0.03	0.22× 0.05 × 0.03
Radiation	Cu K_α (λ = 1.54184)	Cu K_α (λ = 1.54184)	Cu K_α (λ = 1.54184)	Cu K_α (λ = 1.54184)
2Θ range for data collection/°	7.306 to 146.934	6.906 to 147.472	7.068 to 147.292	6.948 to 147.066
Index ranges	−18 ≤ h ≤ 15, −43 ≤ k ≤ 53, −41≤ l ≤ 37	−17 ≤ h ≤ 17, −50 ≤ k ≤ 52, −23 ≤ l ≤ 41	−12 ≤ h ≤ 18, −52 ≤ k ≤ 48, −41 ≤ l ≤ 41	−17 ≤ h ≤ 17, −53 ≤ k ≤ 53, −41 ≤ l ≤ 40
Reflections collected	148791	83443	152041	368403
Independent reflections	42145 [R_{int} = 0.0422, R_{sigma} = 0.0340]	40194 [R_{int} = 0.0625, R_{sigma} = 0.0792]	41905 [R_{int} = 0.0407, R_{sigma} = 0.0320]	40647 [R_{int} = 0.0712, R_{sigma} = 0.0310]
Data/restraints/parameters	42145/244/1900	40194/250/2101	41905/1797/2022	40647/280/1915
Goodness-of-fit on F^2	1.031	1.034	1.058	1.046
Final R indexes [I>=2σ (I)]	R_1 = 0.0795, wR_2 = 0.2335	R_1 = 0.0886, wR_2 = 0.2398	R_1 = 0.0759, wR_2 = 0.2081	R_1 = 0.0797, wR_2 = 0.2062
Final R indexes [all data]	R_1 = 0.0878, wR_2 = 0.2433	R_1 = 0.1102, wR_2 = 0.2594	R_1 = 0.0822, wR_2 = 0.2138	R_1 = 0.0954, wR_2 = 0.2236
Largest diff. peak/hole / e Å^{-3}	3.84/−2.29	5.11/−2.44	2.44/−1.69	2.62/−1.42

S11. References

1 CrystalisPro: Agilent Technologies Ltd: Yarton, Oxfordshire, England; 2015

2 G. M. Sheldrick, *Acta Crystallogr., Sect. A: Found. Crystallogr.*, 2008, **64**, 112–122.

3 O. V. Dolomanov, L. J. Bourhis, R. J. Gildea, J. A. K. Howard and H. Puschmann, *J. Appl Crystallogr.*, 2009, **42**, 339–341.